Controlling Front Position in Catalytic Diffusion–Convection–Reaction Systems

ARTICLE *in* INDUSTRIAL & ENGINEERING CHEMISTRY RESEARCH · MARCH 2002

Impact Factor: 2.59 · DOI: 10.1021/ie0107082

3 AUTHORS:

Moshe Sheintuch
Technion - Israel Institute of Technology
262 PUBLICATIONS **4,717** CITATIONS
SEE PROFILE

Yelena Smagina
Technion - Israel Institute of Technology
20 PUBLICATIONS **75** CITATIONS
SEE PROFILE

Olga Nekhamkina
Technion - Israel Institute of Technology
63 PUBLICATIONS **440** CITATIONS
SEE PROFILE

Controlling Front Position in Catalytic Diffusion−Convection−Reaction Systems

Moshe Sheintuch,* Yelena Smagina, and Olga Nekhamkina

Department of Chemical Engineering, Technion, Haifa, Israel 32000

The stabilization of front solutions in reaction−convection−diffusion systems is studied by presenting a hierarchical picture of one-dimensional models that admit such solutions and that may be approximately reduced to a two-variable system incorporating a fast and diffusing activator and a slow and localized inhibitor. The control procedures are studied using the reduced models with approximate (polynomial) kinetics, for which case some analytical results may be derived, as well as the full model of an exothermic reaction in a fixed bed, where only numerical results are available. In the former case, we reduce the partial differential equation model to a simple ODE that describes the front position, accounting for effects of convection, system size, and boundary conditions; linear stability analysis of the stationary-front solution without and with control was conducted as well. We consider the simplest control strategy based on a single sensor, placed at the front position, and a single space independent actuator that affects one of the parameters or the flow rate or the feed (boundary) conditions; mathematically, these three modes affect the source function, the convective term, or the boundary conditions. The front could be controlled at its stationary position, using either the first or second mode, but the third mode generally failed to stabilize the system. The reduced system was found to be a useful learning tool for the analysis of the full model.

1. Introduction

The purpose of this work is to study the problem of pattern stabilization in a reaction−convection−diffusion system, with exothermic reactions of generic kinetics, by presenting a hierarchical picture of one-dimensional models that admit front solutions, deriving approximate solutions for the dynamics of such motion, and applying these approximations in various control procedures. The stability analysis is based on model reduction to a model that follows the front positions using approximate solutions of the front velocity and front interaction. This approach is different from the traditional approach in chemical engineering problems of control of distributed systems, which typically employs a finite, preferably small, discretization of the underlying partial differential equations (PDEs) typically using trigonometric series and applying the Galerkin method.[1,2] Such a general approach was used for the stabilization of front-like solutions of reaction−diffusion and reaction−diffusion−convection systems,[3,4] but it does not use the specific wave property of the front-like solutions and, hence, it does not provide any insight in designing the control system.

Stationary fronts are key elements in the emergence of stationary or moving patterns, and following their motion is a natural approach for model reduction as described below. We have recently applied the suggested approach to analyze the stability of one-dimensional patterns in one- or two-variable reaction−diffusion systems.[5] A stationary single front or a pattern with n fronts was shown to be typically unstable because of the interaction between fronts. The two simplest control modes, global control and point-sensor control (or pinning; both are defined below), will arrest a front in a single-variable problem because both control modes, in fact, respond to the front position. In a two-variable system incorporating a localized inhibitor, in the domain of bistable kinetics, global control may stabilize a single front only in sufficiently short systems while point-sensor control can arrest such a front in a system of any size, provided it is situated sufficiently close to the front. In systems with uncertainty of the parameters or when a slow deactivation occurs, the front position may vary from its setpoint, and the latter approach may fail. Neither of these control modes can stabilize an n-front pattern, in either one- or two-variable systems, and that task calls for a distributed actuator.

The problem of finite-dimensional control of systems that are described by PDEs has been attracting considerable attention, especially for applications of reaction and diffusion[6,7] and fluid-flow processes.[8−11] The approach taken here is different from that applied in most studies. The dissipative nature of the underlying PDEs, and numerous studies of the spectrum of the eigenvalues of the linearized system, suggests that the long-term dynamics is low-dimensional. Several approaches for model reduction have been suggested; recent approaches were based on the central manifold theorem[7] or on approximate inertial manifold[8,10,11] and allowed for low-order controller design for parabolic PDEs. As remarked earlier, the approach taken here is different from that applied in most studies because it uses a reduced model of the PDE by a simple ODE that describes the front position; in that sense it relies on our qualitative understanding of the system dynamics, but it is limited to systems that admit front solutions.

The structure of this work is the following: In the next section we present a general model of a reactor, using a generic first-order and exothermic reaction, and several learning models that can be derived from it for the following three situations: (i) the adiabatic reactor,

* To whom correspondence should be addressed. E-mail: cermsll@tx.technion.ac.il. Fax: 04-8230476.

10.1021/ie0107082 CCC: $22.00
Published on Web 03/26/2002

(ii) the cross-flow reactor, and (iii) the catalytic wire or ribbon. These three situations can be further simplified to a model of the form

$$y_t - y_{zz} + Vy_z = P(y,\theta,\lambda), \quad V(y|_o - y_{in}) = y_z|_o, \quad y_z|_L = 0 \quad (1a)$$

where y is the state variable (typically the temperature), θ is a localized (nondiffusing) variable (catalytic activity) that is described below, and λ is the control variable. The three situations described above differ in the absence or presence of convection ($V = 0$ in the catalytic wire, while $V \neq 0$ in the two reactor models) and in the bistability features of $P(y) = 0$: P is always monostable in the adiabatic reactor and is bistable for the other two situations in the domain of interest. This model can exhibit front solutions that may become unstable because of various interactions. Yet, while analytical results exist for a single front in unbounded systems with a polynomial source function,[12,13] the behavior of a realistic bounded (finite-size) system with several fronts, and arbitrary kinetics, cannot be predicted analytically in most cases. The boundary conditions are the well-accepted Danckwert's conditions, which reduce to no-flux conditions in the catalytic wire case.

We refer to single-variable systems as those with fixed activity ($\theta = 1$), while in two-variable systems, θ is varying; the second variable (θ) is slow and nondiffusing, and its kinetics is described by

$$\theta_t = \epsilon Q(y,\theta) \quad (1b)$$

($\epsilon \ll 1$ is the ratio of time scales). The interaction of the these two variables leads to complex spatiotemporal patterns that were investigated extensively by us, as well as by others, for the three situations described here: Sheintuch and Nekhamkina[14] studied the adiabatic reactor, while Nekhamkina et al.[15,16] studied the cross-flow reactor. Numerous studies of the diffusion−reaction system that represents the catalytic wire were summarized in monographs;[12,13] papers[17,18] studied the catalytic wire under global control.

The control of a stationary front in eq 1 is analyzed in the following section and is compared with a few numerical experiments of the detailed models.

2. Models and Learning Models

Several classes of reactor models can be written in the following form, for a generic first-order activated kinetics, $r = A\theta e^{-E/RT}C_A$, where we have used conventional notation for variables and dimensionless parameters

$$\frac{\partial x}{\partial \tau} + \delta \frac{\partial x}{\partial \xi} - \frac{1}{Pe_C}\frac{\partial^2 x}{\partial \xi^2} = Da\theta(1-x)\exp\left(\frac{\gamma y}{\gamma + y}\right) + \beta_C(x_w - x) = f_1(x,y,\theta)$$

$$Le\frac{\partial y}{\partial \tau} + \delta \frac{\partial y}{\partial \xi} - \frac{1}{Pe_T}\frac{\partial^2 y}{\partial \xi^2} = BDa\theta(1-x)\exp\left(\frac{\gamma y}{\gamma + y}\right) + \beta_T(y_w - y) = f_2(x,y,\theta) \quad (2)$$

x and y are the dimensionless concentration and temperature.[15]

We refer below to three specific models: (i) the familiar homogeneous model of an adiabatic reactor ($\beta_C = \beta_T = 0$ and $\delta \neq 0$); (ii) the cross-flow reactor where we assume dispersion of a reactant along a packed-bed reactor rather than supplying it with the feed ($\beta_C \neq 0$, $\beta_T \neq 0$, and $\delta \neq 0$); cross-flow reactors were recently studied by us;[15,16] this design may be advantageous in several classes of reactions such as in partial-oxidation reactions where a high feed concentration of oxygen leads to poor selectivity while low concentrations limit the rate and conversion; (iii) the catalytic wire, i.e., a system without convection ($\beta_C \neq 0$, $\beta_T \neq 0$, and $\delta = 0$), which is presented here for comparison. By the *homogeneous model* we refer to the assumption that interphase gradients of temperature and concentration are absent and the flow terms are included in the corresponding balances ($\delta = 1$). The Danckwert's boundary conditions are typically imposed on the model

$$\xi = 0, \quad \frac{\partial x}{\partial \xi} = \delta Pe_C(x - x_{in}), \quad \frac{\partial y}{\partial \xi} = \delta Pe_T(y - y_{in}), \quad \xi = 1, \quad \frac{\partial x}{\partial \xi} = \frac{\partial y}{\partial \xi} = 0 \quad (3)$$

and it applies to models i and ii, as well as to model iii with $\delta = 0$.

The main features, relevant to front propagation, of these three models are the following: The catalytic wire admits homogeneous (space-independent) solutions and may admit fronts separating the two stable solutions of $f_1 = f_2 = 0$; in the absence of convection the front may propagate in either direction. Similar features apply to the cross-flow reactor, but convection "pushes" the front downstream. The unique aspect of such a reactor is that sufficiently far from the inlet the system approaches a homogeneous (space-independent) solution. Highly exothermic or highly activated reactions may yield multiple such solutions, and in the distributed system, fronts separating different states may be formed. Another feature unique to this reactor is that under certain conditions the homogeneous state becomes unstable and a branch of stationary patterns emerges. Homogeneous solutions do not exist in an adiabatic reactor, but we find front-like solutions due to reaction and convection which may move in response to feed conditions. Several approximations for the velocity of these fronts have appeared in the literature.[19−21]

We turn now to derive several learning models.

Learning Model I: The Adiabatic Reactor. In its usual form the homogeneous model does not account for mass supply, and if the reactor is adiabatic, $\beta_C = \beta_T = 0$. For most catalytic reactors, we can assume that the solid heat capacity is large ($Le \gg 1$) and that mass-axial mixing is negligible ($Pe_C \to \infty$), so that the fluid mass-balance is reduced to the simple form $dx/d\xi = (1 - x)\theta g(y)$ with

$$g(y) = Da\exp\left(\frac{\gamma y}{\gamma + y}\right)$$

subject to $x(0) = x_{in} = x_0$. Defining

$$\phi = Bx - y \quad (4)$$

we find from eq 2

$$\frac{\partial \phi}{\partial \xi} = -\frac{1}{Pe_T}\frac{\partial^2 y}{\partial \xi^2} + \frac{\partial y}{\partial(\tau/Le)} \quad (5)$$

and after some rearrangement

$$\frac{\partial y}{\partial(\tau/Le)} + \frac{\partial y}{\partial \xi} - \frac{1}{Pe_T}\frac{\partial^2 y}{\partial \xi^2} = P(y,\theta) + G(y,\theta,\xi);$$

$$P(y) = (B - y)\theta g(y);$$

$$G(y,\theta,\xi) = (y_{in} - Bx_o)\theta g(y) - \theta g(y)\frac{\mathrm{d}\int_0^\xi y\,\mathrm{d}\xi}{\mathrm{d}(\tau/Le)} \quad (6)$$

Learning Model II: The Cross-Flow Reactor. Assuming again that $Le \gg 1$ and that mass-axial mixing is negligible ($Pe_C \to \infty$), so that the fluid mass balance is reduced to the simple form

$$\frac{\mathrm{d}x}{\mathrm{d}\xi} = (1 - x)\theta g(y) + \beta_C(x_w - x) \quad (7)$$

subject to $x(0) = x_{in} = x_o$. Define the dimensionless variable with respect to wall conditions so that $x_w = y_w = 0$, and set for the sake of simplicity $\beta_C = 1$. Combine the two balances to find the equation that describe the invariant

$$\frac{\partial \phi}{\partial \xi} + \phi = \frac{\partial y}{\partial(\tau/Le)} + \frac{\partial y}{\partial \xi}(1 - \beta_T) - \frac{1}{Pe_T}\frac{\partial^2 y}{\partial \xi^2} = F(y,y_\xi,y_{\xi\xi});$$

$$\phi = Bx - \beta_T y \quad (8)$$

Expressing ϕ as

$$\phi = \phi_0 e^{-\xi} + \int_0^\xi e^{-(\xi-\xi')}F(\xi')\,\mathrm{d}\xi' \quad (9)$$

and integrating terms such as $\int e^{\xi'} y_\xi\,\mathrm{d}\xi$, etc., yields

$$Bx = \beta_T y + (Bx_o - \beta_T y_o)e^{-\xi} + \tilde{G}(\xi)$$

$$\tilde{G}(\xi) = e^{-\xi}\left[\left(1 - \beta_T + \frac{1}{Pe_T}\right)\left(ye^{\xi} - y_o - \int_0^\xi e^{\xi'} y\,\mathrm{d}\xi'\right) - \frac{1}{Pe_T}\left(\frac{\partial y}{\partial \xi}e^{\xi} - \left.\frac{\partial y}{\partial \xi}\right|_o\right) + \frac{\mathrm{d}}{\mathrm{d}(\tau/Le)}\int_0^\xi e^{\xi'} y\,\mathrm{d}\xi'\right] \quad (10)$$

Substituting x into the original enthalpy balance, after substituting the boundary conditions and neglecting terms multiplied by $1/Pe_T$ with respect to similar terms multiplied by unity, yields, after rearrangement

$$\frac{\partial y}{\partial(\tau/Le)} + \frac{\partial y}{\partial \xi} - \frac{1}{Pe_T}\frac{\partial^2 y}{\partial \xi^2} = P(y) + G(y,\xi);$$

$$P(y) = [B - y - (\beta_T - 1)y]\theta g(y) - \beta_T y$$

$$G(\xi) = (y_{in} - Bx_o)e^{-\xi}\theta g(y) + (1 - \beta_T)\theta g(y) \times \left[\int_0^\xi e^{-(\xi-\xi')} y\,\mathrm{d}\xi' - y\right] - \theta g(y)\frac{\mathrm{d}}{\mathrm{d}(\tau/Le)}\int_0^\xi e^{-(\xi-\xi')} y\,\mathrm{d}\xi' \quad (11)$$

Note that with appropriate inlet conditions the system attains a homogeneous steady state, $y = y_s$.

Learning Model III. *A catalytic wire* exposed to a stream of reactants with fixed fluid concentration ($x_w = 0$ when properly defined) and temperature ($y_w = 0$) is described by eq 2 with no flow ($\delta = 0$) and no mass diffusion ($Pe_C = \infty$) and is subject to no-flux boundary conditions at its edges. Now, because the thermal response is slow (large Le), we can assume the mass balance in eq 2 to be in a pseudo steady state and substitute its solution into the enthalpy balance to achieve a single-variable reaction−diffusion equation

$$Le\frac{\partial y}{\partial \tau} - \frac{1}{Pe_T}\frac{\partial^2 y}{\partial \xi^2} = B\frac{\beta_C \theta g(y)}{\beta_C + \theta g(y)} - \beta_T y \equiv P(y,\theta) \quad (12)$$

for which fronts may exist when $f_1 = f_2 = 0$ is bistable. In a very long system (or equivalently large Pe_T; note that eq 12 is written for a system of size unity), we can impose fronts that separate the upper (y_+) and lower (y_-) steady states. Some well-known properties of such solutions are reviewed below.

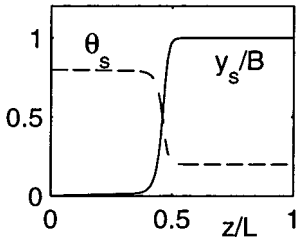

Figure 1. Typical temperature (y_s) and activity (θ_s) profiles in a stationary solution (profiles were calculated for an adiabatic reactor, but similar profiles exist for other situations discussed here).

Learning Model IV. Now we simplify the three models above to one general model so that we can study the qualitative properties of fronts in such a system below. After rescaling time ($\tau Da/Le \to t$) and space ($\xi^2 DaPe_T \to z^2$), while assuming $G(y,\xi) = 0$ in learning models I and II, we derive eq 1 with $V = (Pe_T/Da)^{1/2}$. Note that $G(y,\xi)$ has two contributions: one due to inlet conditions and another due to the changes in concentration beyond its adiabatic relation with temperature. The first effect decays with the distance from the inlet; the second effect may be important in the vicinity of the front, and we will return to assess its importance later. While we are aware that in the process we may lose certain features, eq 1 retains the ability to admit front solutions and demonstrates the correct dependence of front velocity on the parameters. Now, $P(y) = 0$ may be bistable for models II and III, but it is unique for model I, while $V = 0$ in model III. In the domain where $P = 0$ is bistable, models II and III exhibit front solutions. Model I exhibits such a solution for a certain range of V. The properties of front velocity are outlined below. We are interested in instabilities due to the interaction of the front with a slow process of changing activity, that is described by eq 1b (see Sheintuch and Shvartsman[22] for a detailed description).

3. Qualitative Analysis

In this section we try to present a qualitative analysis based on a simplified model of control of a diffusion−convection−reaction system, by reducing the PDE model to a simple ODE that describes the front position, using an approximate expression for the front velocity: We note that for $\tau_\theta \gg Le$ ($\tau_\theta = \epsilon^{-1}$) the activity profile is too slow to respond to the front motion, and because we are interested in small deviations from the setpoint, we can consider the activity profile to be frozen at its steady-state position, $\theta = \theta_s(y_s)$. The typical steady y_s and θ_s profiles are presented in Figure 1. The instability stems

from the anticlinal distribution of the two: a perturbation of the front to the left will encounter higher activity, which will enhance its velocity, etc. Thus, for short times the model can be reduced to the following form:

$$y_t - y_{zz} + Vy_z = P(y,\theta_s(z),\lambda), \quad V(y|_o - y_{in}) = y_z|_o, \quad y_z|_L = 0 \tag{13}$$

where we have singled out one parameter (λ) that will be later used for control purposes. Assuming the existence of a shape-preserving front, its position (Z_f) follows from the front velocity (c)

$$dZ_f/dt = -c(\theta_s(Z_f),\lambda) \tag{14}$$

We will always refer to fronts that separate a low state on the left from a high one on the right. We assign positive velocity to an expanding high state. The control variable λ affects the front velocity, but large perturbations of λ may destroy the front altogether if $P(y,\theta_s(z),\lambda)$ is bistable.

While certain analytical results exist for the front velocity in the unbounded diffusion−reaction system of the form $y_t - y_{zz} = P(y)$, with a bistable source function and constant parameters, here we need to correct the front velocity for three terms: (i) the convective (or rather advective) flow, (ii) the finite size and the boundary conditions, and (iii) the spatially varying activity.

To find the velocity under the effect of convection, assume that the system is unbounded, and defining a new coordinate moving with the front

$$\zeta = z - c_\infty t \tag{15}$$

we find its shape from

$$(V - c_\infty)y_\zeta - y_{\zeta\zeta} = P(y,\theta_s,\lambda) \tag{16}$$

Edge effects on front velocity decay exponentially with the front distance from the edges, and for the sake of simplicity, we assume that the separation is sufficiently large to ignore it. This equation is similar to that derived for a diffusion−reaction problem (i.e., in the absence of convection), except that the front velocity is corrected by the fluid velocity, $-c_\infty = -c_{\infty,V=0} + V$. While analytical solutions exist only in a few cases (notably polynomial kinetics and piecewise linear P), we can derive certain results from the theory of diffusion−reaction fronts. We can integrate eq 16 (after multiplying by $dy/d\zeta$) as

$$(V - c_\infty)\int_{-\infty}^{-\infty} y_\zeta^2\, d\zeta - \frac{1}{2} y_\zeta^2\Big|_{-\infty}^{\infty} = \int_{y_-}^{y_+} P(y,\theta_s,\lambda)\, dy \tag{17}$$

Note that the first integral on the left is positive, the second term vanishes for an unbounded system with no flux conditions, and the integral on the right determines the sign of $(c_\infty - V)$. Thus, in an unbounded system with convection

$$dZ_f/dt = -c_\infty(\theta_s(Z_f),\lambda) = -c_{\infty,V=0} + V \tag{18}$$

To study the effect of feed conditions, we discuss now the interaction with the edges: Assume the system to be sufficiently large so that fronts of constant speed and shape develop and move. Now, to find the interaction with the walls, where no-flux conditions apply, let us assume the existence of two fronts: one at $z = Z_{f1}$ separating a "cold" zone on the left from a "hot" one and another, its mirror image, at Z_{f2}. The corresponding solutions, in the absence of a second front, would have been $y_1 = y_\infty(z - Z_{f1})$ and $y_2 = y_\infty(Z_{f2} - z)$ where y_∞ is the solution for an unbounded system. A reasonable approximation of a pulse composed of two mirror-image fronts is

$$y(\zeta) = y_1(\zeta;Z_{f1}) + [y_2(\zeta;Z_{f2}) - y_+] \tag{19}$$

because it describes correctly each front individually, as their separation diverges to infinity. The velocity of an ascending front can be generalized to account for interactions on the left and the right[5]

$$c - c_\infty = \alpha_- e^{2p_-Z_l} - \alpha_+ e^{-2p_+Z_r} \tag{20}$$

where Z_l and Z_r are the distances (in an absolute value) to the closest boundaries on the left and right, respectively, and $p_\pm$ ($p_+ > 0$, $p_- < 0$) are the eigenvalues of the linearized diffusion−reaction equation (16). Obviously, the boundaries effect decline exponentially.

The boundary condition used here (eq 1) is different than the no-flux condition used to develop eq 20, but we can find an imaginary boundary that satisfies this boundary condition. To do that, note that far from the front the profile varies exponentially like $\exp[p(z - Z_{f1})]$ and implementation in eq 19 yields

$$y - y_- = C(e^{p(z-Z_1)} + e^{p(Z_2-z)}) \tag{21}$$

where C is a constant and $p = -p_-$ is the eigenvalue at the lower state. Applying now the boundary condition (eq 1a), we find the location of the imaginary boundary from

$$e^{pZ_{f2}} = -\frac{V(y_- - y_{in})}{C(V + p)} + \frac{p - V}{p + V} e^{-pZ_{f1}} \tag{22}$$

Let us analyze the boundaries effect: When feed conditions coincide with the lower state ($y_- = y_{in}$), we can distinguish between three cases: When $V = 0$, the boundary conditions reduce to no flux and $Z_{f1} = -Z_{f2}$ as we expect from the reaction−diffusion system.[5] When $V < p$, we can find the imaginary boundary, and it shifts to the left with increasing V, reaching $-\infty$ as $V = p$. The boundary does not exist when $V > p$. Similar boundaries can be determined when $y_- \neq y_{in}$, but it requires the estimation of C. For learning model IV with simple polynomial kinetics, we estimate that $C \subset [-y_-, -2y_-]$. Substituting eq 22 into eq 20, we obtain the front velocity. We will return to this approach later.

To express the effect of varying catalytic activity on front velocity, we assume $c(\theta(Z_f))$ to be determined by the local conditions.

We turn now to consider several control strategies. We consider the simplest strategies based on a single sensor and a single space-independent actuator. We can attempt to arrest the front by manipulating a certain operating condition (λ) or by affecting the flow rate or the inlet conditions: For each of this strategies, we can use a control based on a single measurement, either at a preset point or of an average property. These are technically the simplest possible designs, and we refer to them as point-sensor (or pinning) control and global control, respectively. We need to develop a linearized model for front velocities.

We proceed by assuming that the edge effects are negligible and focus on the effect of the parameters. Now the front is stationary for a certain $c_{s,V=0}(\theta_s,\lambda_s) = V$, that is, under conditions that counteract the convective force. Expand now

$$c_{V=0}(\theta_s,\lambda) = c_{s,V=0}(\theta_s(Z_f),\lambda_s) + \left(\frac{\partial c_s}{\partial \theta}\right)_f(\theta_s(Z_f) - \theta_s(Z_s)) + \frac{\partial c_s}{\partial \lambda}(\lambda - \lambda_s) \quad (23)$$

to find the dependence of the front position on activity and on the control variable. Here the subscript f denotes the front position. Because θ is assumed to be frozen for the short perturbation times we consider, we can write

$$\theta_s(Z_f) - \theta_s(Z_s) = \left(\frac{\partial \theta_s}{\partial z}\right)_f(Z_f - Z_s) \quad (24)$$

Moreover, gradients in y and θ are related by

$$\left(\frac{\partial \theta_s}{\partial z}\right)_f = -\frac{Q_y}{Q_\theta}\left(\frac{\partial y}{\partial z}\right)_f \quad (25)$$

where Q_y and Q_θ are evaluated at the setpoint (Q is defined in eq 1b).

Consider now control strategies based on λ: In the point-sensor approach (Z^* = the sensor position)

$$\lambda - \lambda_s = K[y(Z^*) - y_s(Z^*)] \quad (26)$$

We show now that this control responds to changes in the front position. Assuming a perturbation that displaces the front position to Z_f without changing its shape, $y(Z^*) = y(Z_f) + (\partial y/\partial z)_f (Z^* - Z_f)$; hence, $y_s(Z^*) = y_s(Z_s) + (\partial y/\partial z)_s (Z^* - Z_s)$, and

$$\lambda - \lambda_s = -K(\partial y/\partial z)_f(Z_f - Z_s) \quad (27)$$

Thus, from eqs 18 and 23−27, we can approximate the front motion, under control and for small perturbations, as

$$-\frac{dZ_f}{dt} = c_s(\theta_{fs},\lambda_s) - V + \left(\frac{\partial c_s}{\partial \theta}\right)_f\left(\frac{\partial \theta_s}{\partial z}\right)_f(Z_f - Z_s) - K\frac{\partial c_s}{\partial \lambda}\left(\frac{\partial y}{\partial z}\right)_f(Z_f - Z_s) \quad (28)$$

and conclude that a sufficiently large K will always stabilize the front.

In the global-control approach, $\lambda - \lambda_s = K(y_s - \langle y\rangle)$, the control responds to the changes in the average temperature due to changing the front position by changing λ, which, in turn, affects the average temperature as well as the front velocity. Assuming perfect global control (infinite K), we may satisfy the control condition without sufficiently affecting the velocity and the control will fail. To show that, assume perfect control that attempts to maintain the spatially averaged temperature at y_s. If y_- and y_+ are the edge positions and the front is narrow, then the average temperatures at the set and perturbed positions follow:

$$y_-(\lambda_s)(Z_s) + y_+(\lambda_s)(L - Z_s) = \langle y_s\rangle_L$$
$$y_-(\lambda)(Z_f) + y_+(\lambda)(L - Z_f) = \langle y_s\rangle_L \quad (29)$$

Now, expanding $y_\pm(\lambda) = y_\pm(\lambda_s) + (\partial y/\partial\lambda)_f (\lambda - \lambda_s)$ and rearranging yield

$$\lambda - \lambda_s = (Z_f - Z_s)\frac{y_+(\lambda_s) - y_-(\lambda_s)}{\frac{\partial y_-}{\partial \lambda}Z_f + \frac{\partial y_+}{\partial \lambda}(L - Z_f)} \quad (30)$$

The control effect is limited, therefore, by the term on the right, which may or may not be sufficient to stabilize the front, depending on the parameters and the destabilizing gradient of θ. In the symmetric case where $\partial y_-/\partial\lambda = \partial y_+/\partial\lambda$ (as in the cubic source function; see below), the apparent gain declines like $1/L$, and this control fails.

We turn now to study the other actuators.

Convection has two effects in this simplified model: It linearly affects the front velocity (eq 18), and it changes the boundary effect on the front (eqs 20 and 22). Substituting eq 22 into eq 20, we obtain

$$\frac{dZ_{f1}}{dt} = -c_{\infty,V=0} + V - \alpha_-\left[\frac{V(y_{in} - y_-)}{C(V+p)}e^{-pZ_f} + \frac{p - V}{p + V}e^{-2pZ_f}\right] + \alpha_+ e^{-2p(L-Z_f)} \quad (31)$$

Again, using a control law of the form

$$V - V_s = K(y(Z^*) - y_s(Z^*)) \sim -K(\partial y/\partial z)_f(Z_f - Z_s) \quad (32)$$

we can approximate the required gain; specifically, when the front is sufficiently far from the boundaries, we find for small perturbations

$$-\frac{dZ_f}{dt} = c_s(\theta_{fs}) - V_s + \left(\frac{\partial c}{\partial \theta}\right)_f\left(\frac{\partial \theta}{\partial z}\right)_f(Z_f - Z_s) - K\left(\frac{\partial y}{\partial z}\right)_f(Z_f - Z_s) \quad (33)$$

suggesting that an actuator based on the flow rate may be useful.

The third actuator to consider is based on feed conditions. Changing the feed conditions will affect y_{in} and, consequently, will affect the front velocity (eq 31). We cannot ignore now the effect of boundaries (eq 31), but obviously the gain should be of order $\exp(pZ)$, suggesting that it may be practical only for fronts that are not removed from the entrance. Control law of the form

$$y_{in} - y_{in,s} = K(y(Z^*) - y_s(Z^*)) \sim -K(\partial y/\partial z)_f(Z_f - Z_s) \quad (34)$$

can stabilize the system, subject to certain limitations that we discuss below.

The three control strategies were shown to be adequate for controlling small perturbations in the front position. Yet, large perturbations of the fronts will cause λ to exceed the bistability domain of $P = 0$ and consequently to switches of y at one edge of the system, which will result in a flip of the whole profile as we show below. Thus, perturbation in λ should be limited so as not to exceed this threshold.

4. Numerical Simulations

In this section, we verify the conclusions above by conducting several simulations. We use two models: (i)

learning model IV with simple polynomial kinetics, for which we can find analytical expressions for the front velocity; (ii) model I, which is a detailed model and in which fronts are somewhat different from those in bistable systems, as we explain in the Introduction.

Learning Kinetics. Let us study the two-variable system

$$y_t - y_{zz} + Vy_z = -(y^2 - 1)(y - a) + \theta + \lambda = P(y,\theta,\lambda),$$

$$\theta_t = \epsilon(-y\gamma - \theta) = Q(y,\theta)$$

$$V(y|_o - y_{in}) = y_z|_o, \quad y_z|_L = 0 \tag{35}$$

composed of eq 1a with a cubic source function and a simple linear Q function (eq 1b). For fixed $\theta + \lambda = 0$, the unbounded system (35) admits the following analytical solution for the profile and front velocity:[13]

$$y = \tanh[(z - Z_f)/\sqrt{2}], \quad c_\infty = V + \sqrt{2}a$$

Evidently, the front is stationary when

$$a = -V/\sqrt{2} \tag{36}$$

Two-variable system (35) admits the steady-state analytical solution of the same form:

$$y = \sqrt{1-\gamma}\,\tanh[(z - Z_f)\sqrt{0.5(1-\gamma)}], \quad \theta = -\gamma y \tag{37}$$

if the relation (36) is satisfied and the control variable is assigned as

$$\lambda = \gamma a \tag{38}$$

Note that the solution (eq 36) exists if $|a| < |y_\pm| = \sqrt{1-\gamma}$, i.e., $V < \sqrt{2(1-\gamma)}$ and the source function $P(y,\theta,\lambda)$ is bistable if $a - \sqrt{a^2+3} > -3\sqrt{1-\gamma}$.

We argue now why the proposed learning kinetics represents well the actual kinetics. This form can be derived from eq 1 by linearizing $P(y,\theta)$ of eq 6 or eq 11 with respect to θ and replacing $g(y)$ in P by

$$g'(y) = Da^*(a + y^2) \tag{39}$$

where the two parameters are obtained by matching $g(y)$ and $g'(y)$ at the lowest temperature ($y = 0$; i.e., $Da = aDa^*$) and at the adiabatic temperature rise ($y = B$). Note that Da^*, t, and y were rescaled; in the resulting cubic $P(y)$, the quadratic term can be eliminated by rescaling y.

In the catalytic wire problem, because the source function $P(y)$ is bistable within a certain domain, we replace it with a cubic source function that shows qualitatively similar behavior, and after redefining the time and length scales and the variable (y), we arrive at the reaction−diffusion equation above (with $V = 0$). The control of this problem has been extensively investigated.[2,3]

Linear stability analysis of system (35) was conducted by spectral methods using the eigenfunctions of the problem (see Appendix). Analysis of the leading eigenvalues (see Figure 2) shows that the eigenvalues converge with the truncation order of the Galerkin series when using $N \sim 10$ or more terms.

As stated in the qualitative analysis, the control is most sensitive when the sensor is positioned at the front. That is verified in Figure 3, which displays the dependence of the leading eigenvalues on the additive-control gain (K) for a sensor positioned at the front ($Z_f = 10$) or away from it: Positioning the sensor at $Z^* = 7$ fails to stabilize the front. In most simulations below the sensor is positioned at the front. As stated

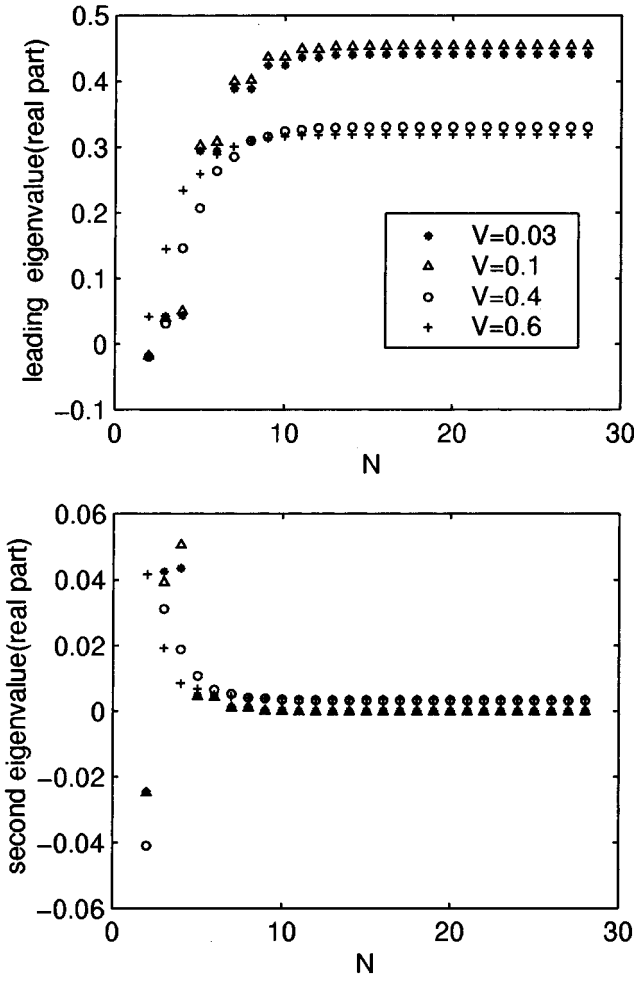

Figure 2. Evaluation of the truncation order N of the linearized system (eq 35) for $L = 20$, $\gamma = 0.45$, $\epsilon = 0.01$, and various V. The first and second eigenvalues are plotted vs the order of the Galerkin truncation. Linearization is performed around the analytical steady front solution (eq 37).

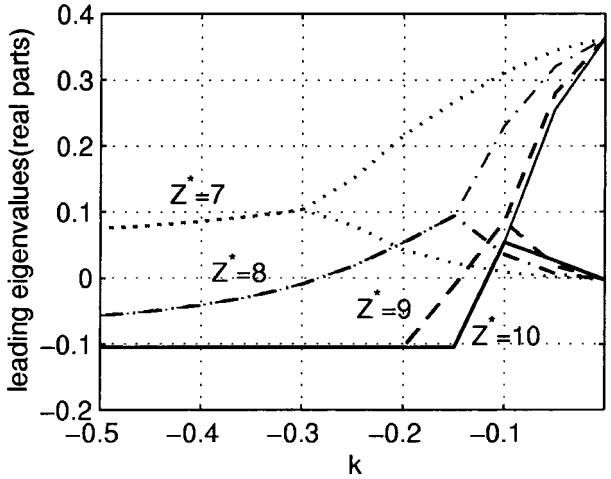

Figure 3. Effect of the sensor position (Z^*) on the leading eigenvalues of the closed-loop system for the additive-control action (eq 35 with $V = 0.03$, $\epsilon = 0.1$, $L = 20$, $\gamma = 0.45$, and $y_{in} = -0.74$).

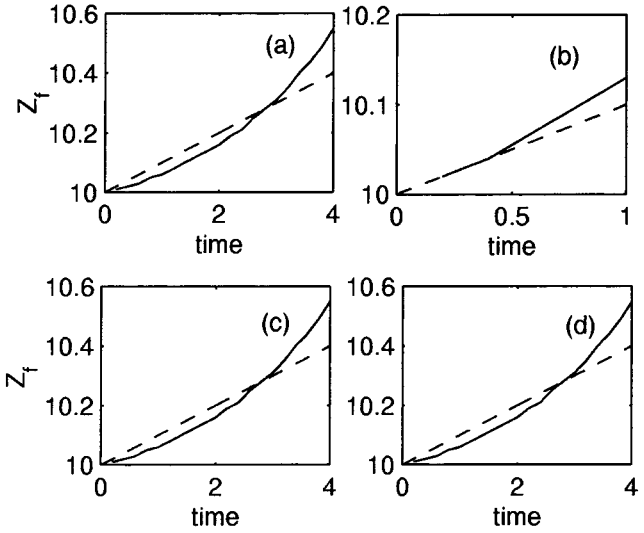

Figure 4. Comparison of the front dynamics estimated by the simulation of the PDEs (eq 35; solid line) or the approximate system (eq 31; broken line) [$\gamma = 0.45$, $\epsilon = 0.01$, $L = 20$: (a) $V = 0.05$, $y_{in} = y_-$; (b) $V = 0.1$, $y_{in} = y_-$; (c) $V = 0.05$, $y_{in} > y_-$; (d) $V = 0.05$, $y_{in} < y_-$].

earlier, this may lead to failure of the controller when the activity or the parameters vary.

The scalar gain coefficient K can be estimated numerically, using the linearized system, or approximately, using the simplified model of a front position (see the Appendix). The adequacy of model reduction is demonstrated in Figure 4, which compares the simulated front position of eq 35 ($a = 0$) with the solution of the approximated equation for the front position (eq 31). Good agreement between the two is demonstrated.

The dynamics of the parameter (or additive) actuator (i.e., manipulating λ) and of the flow-rate actuator (manipulating V) are analyzed below: Figure 5a displays the dynamics of two types of parameter control using either a proportional ($\lambda = K[y(Z^*) - y_s(Z^*)]$, broken line) or proportional−integral (PI; solid line) control, of the form

$$\lambda = K_1[y(Z^*) - y_s(Z^*)] + K_2 q; \qquad dq/dt = [y(Z^*) - y_s(Z^*)] \quad (40)$$

The latter approach ensures a better response and a smaller static error. Similarly, Figure 6a displays the dynamics of proportional flow-rate control ($V - V_s = K[y(Z^*) - y_s(Z^*)]$) with either insufficient gain ($K = -1$; critical gain was evaluated to be -2) or with a sufficiently large gain ($K = -4$). Figure 6b compares proportional and PI control

$$V - V_s = K_1[y(Z^*) - y_s(Z^*)] + K_2 q, \qquad dq/dt = [y(Z^*) - y_s(Z^*)]$$

showing the latter to be better.

Parts b and c of Figure 5 demonstrate the necessity of restricting the magnitude of the control variable for keeping it within the domain of bistability; otherwise, when large initial perturbations are imposed, with a resulting large feedback, a flip of the profile is observed (Figure 5c).

Detailed Models. The control design for a detailed model of the cross-flow reactor was studied by Panfilov and Sheintuch,[4] and it typically verifies the strategies

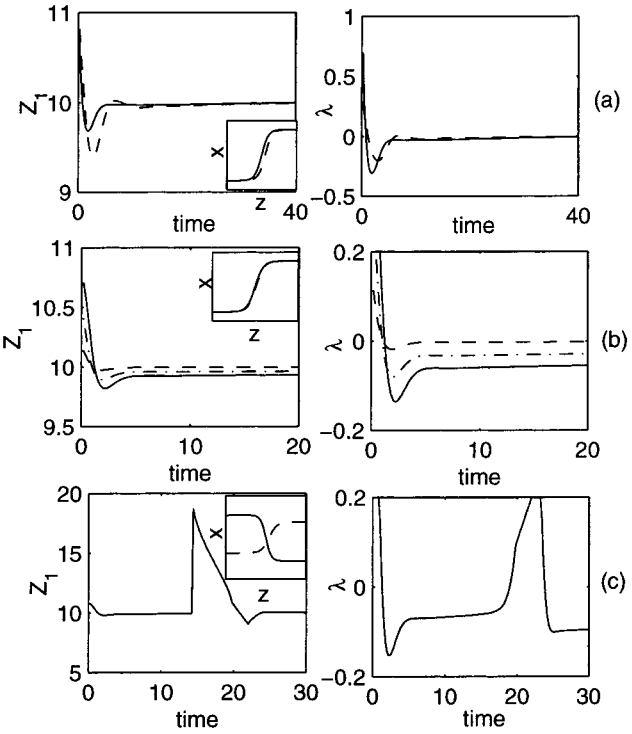

Figure 5. Response of the closed-loop system (eq 35) using a parameter (or additive) actuator to an initial perturbation. The figure presents the front position Z_f (column 1) and the control variable λ (column 2) and the initial (inset, dashed line) and final (inset, solid line) front profiles. (a) Comparison of the P regulator with $K = -1$ (dashed line) and the PI regulator with $K_1 = -1$ and $K_2 = -2$ (solid line; other parameters are $\epsilon = 0.1$, $V = 0.5$, $L = 20$, $y_{in} = -0.74$). (b and c) Influence of the magnitude in front-position perturbations: While moderate perturbations (b: $\Delta Z_f = 0.1$, 0.5, and 0.7—broken, dash-dotted, and solid lines, respectively) can be controlled, large perturbations (c: $\Delta Z_f = 1$) result in large λ and flipping of the profile (P regulator ($K = -2$), $\epsilon = 0.01$; other parameters are as in Figure 3).

developed here using learning model IV with simplified cubic kinetics.

We study now the stabilization of the adiabatic reactor (eqs 1b and 2), applying the same procedures tested for the other cases and using approximated expressions for front velocities. We adopt here a simple linear expression that assumes that deactivation occurs faster at higher temperatures and at higher activities and that it is independent of reactant concentration, so the dimensionless form of the catalytic activity variation is $\theta_\tau = \epsilon(a_\theta - b_\theta\theta - y)$ where a_θ and b_θ are constants. Recall that the detailed model of an adiabatic reactor differs from the models discussed above, because the system does not admit a homogeneous solution but admits a front solution because of interaction of reaction and convection. We tested the three types of actuators: (i) In V control, we manipulated $\delta = 1 - \lambda$, where $\lambda = K[y(Z^*) - y_s(Z^*)]$. (ii) In parameter control, we manipulated $B = B_o - \lambda$; recall that B is proportional to the feed concentration. (iii) In boundary control, we varied the feed concentration, $x_{in} = x_{in,o} - \lambda$ and the feed temperature $y_{in} = y_{in,o} - \lambda$.

The first two types of the control were successful in stabilizing the system (Figure 7a). The efficiency of the boundary control depends on the choice of the manipulated variables: x_{in} control is effective (Figure 7b), while y_{in} control failed to stabilize the front (Figure 7c) for the specified conditions. The appropriate gain values employed in V, B, and x_{in} controls assured a stable response

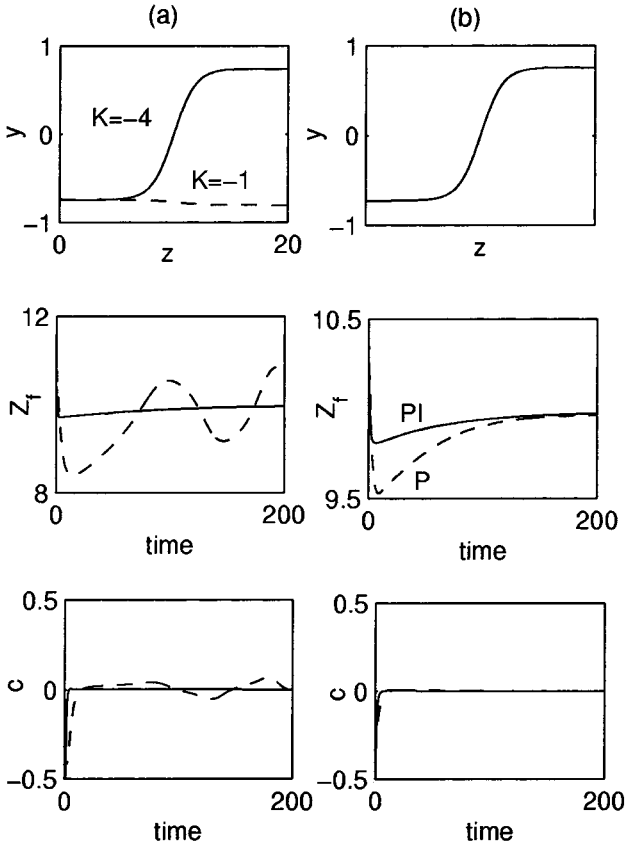

Figure 6. Response of the closed-loop system using the flow-rate control to an initial perturbation [$V_o = 0.1$, $\epsilon = 0.01$; other parameters are as in Figure 3; $Z^* = Z_f = 10$]. The figure presents the final front profiles (row 1), the front position Z_f (row 2), and the velocity c (row 3): (a) P regulator with the insufficient gain $K = -1$ (dashed line) and sufficient gain $K = -4$ (solid line); (b) P regulator with gain $K = -2$ (dashed line) and PI regulator with gains $K_1 = K_2 = -2$ (solid line).

(Figure 7). As the gain declines, the system oscillates around the unstable position.

5. Conclusion

The stabilization of front solutions in reaction−convection−diffusion systems is studied by presenting a hierarchical picture of one-dimensional models that admit such solutions: the homogeneous model of an adiabatic reactor, the cross-flow model with feeding of a reactant along a packed bed, and the catalytic wire. These models differ in the absence or presence of a homogeneous solution and in the absence or presence of convection. We showed that the three models may be approximately reduced to a two-variable system incorporating a fast and diffusing activator and a slow and localized inhibitor. The control procedures are studied using the reduced models with approximate (polynomial) kinetics, for which case some analytical results may be derived. The main qualitative properties of the fronts may be captured by the learning model, which demonstrates the correct dependence of the front velocity on the parameters.

In analyzing the learning model, we reduce the PDE model to a simple ODE that describes the front position, accounting for effects of convection, system size, and the boundary conditions; linear stability analysis of the stationary-front solution without and with control was conducted as well. This solution allows one to estimate qualitatively the impact of different parameters and thus to construct the suitable control tools and for the case of very slow inhibitor to predict the system dynamics with sufficient accuracy.

We consider the simplest control strategy based on a single sensor, placed at the front position, and a single space-independent actuator that affects either one of the parameters or the flow rate or the feed (boundary) conditions; mathematically, these three modes affect the source function, the convective term, or the boundary conditions. The front could be controlled at its stationary position, using either the first or second mode, but the third mode generally failed to stabilize the system. The reduced system was found to be a useful learning tool for the analysis of the full model.

Acknowledgment

Work was supported by the Israel Science Foundation and by the U.S.−Israel Binational Science Foundation. Y.S. and O.N. are partially supported by the Center for Absorption in Science, Ministry of Immigrant Absorption, State of Israel. M.S. is a member of the Minerva Center of Nonlinear Dynamics.

Appendix

Linear Stability Analysis of Equation 35 and Control Design. The linearization of eq 35 with constant V around $y_s = y_s(z)$ and $\theta_s = \theta_s(z)$, the steady-state solution for $\lambda = 0$, yields

$$\bar{y}_t + V\bar{y}_z - \bar{y}_{zz} = \frac{\partial P}{\partial y}(y_s,\theta_s)\,\bar{y} + \bar{\theta} + \lambda \qquad \text{(A1)}$$

$$\bar{\theta}_t = -\epsilon\gamma\bar{y} - \epsilon\bar{\theta} \qquad \text{(A2)}$$

where $\bar{y} = \bar{y}(z,t) = y(z,t) - y_s$ and $\bar{\theta} = \bar{\theta}(z,t) = \theta(z,t) - \theta_s$ are the deviations.

We substitute the feedback control in eq A1: $\lambda(t) = K\bar{y}(Z^*,t)$, where K is a constant gain coefficient and $Z^* \in [0, L]$ is the position of the sensor. We lump eqs A1 and A2 by expanding the deviations $\bar{y}(z,t)$, $\bar{y}(Z^*,t)$, and $\bar{\theta}(z,t)$ as

$$\bar{y}(z,t) = \sum_i a_i(t)\,\phi_i(z), \quad \bar{y}(Z^*,t) = \sum_i a_i(t)\,\phi_i(Z^*), \quad \bar{\theta}(z,t) = \sum_i b_i(t)\,\phi_i(z) \qquad \text{(A3)}$$

where the orthonormal basis functions $\phi_i(z)$ are the eigenfunctions of the problem: $\phi_{izz} - V\phi_{iz} = -\lambda_i\phi_i$ with the eigenvalues $\lambda_i = \sigma_i^2 + V^2/4$. Eigenfunctions $\phi_i(z)$ and adjoint eigenfunctions $\phi_i^a(z)$ are defined as

$$\phi_i(z) = \Theta_i e^{0.5Vz}\left[\cos(\sigma_i z) + \frac{V}{2\sigma_i}\sin(\sigma_i z)\right] \qquad \text{(A4)}$$

$$\phi_i^a(z) = \Theta_i e^{-0.5Vz}\left[\cos(\sigma_i z) + \frac{V}{2\sigma_i}\sin(\sigma_i z)\right], \quad \phi_i^a(z) = \phi_i(z)\,e^{-Vz} \qquad \text{(A5)}$$

$$\Theta_i = \frac{1}{\left(\int_0^L\left(\cos(\sigma_i z) + \frac{V}{2\sigma_i}\sin(\sigma_i z)\right)^2 dz\right)^{0.5}} \qquad \text{(A6)}$$

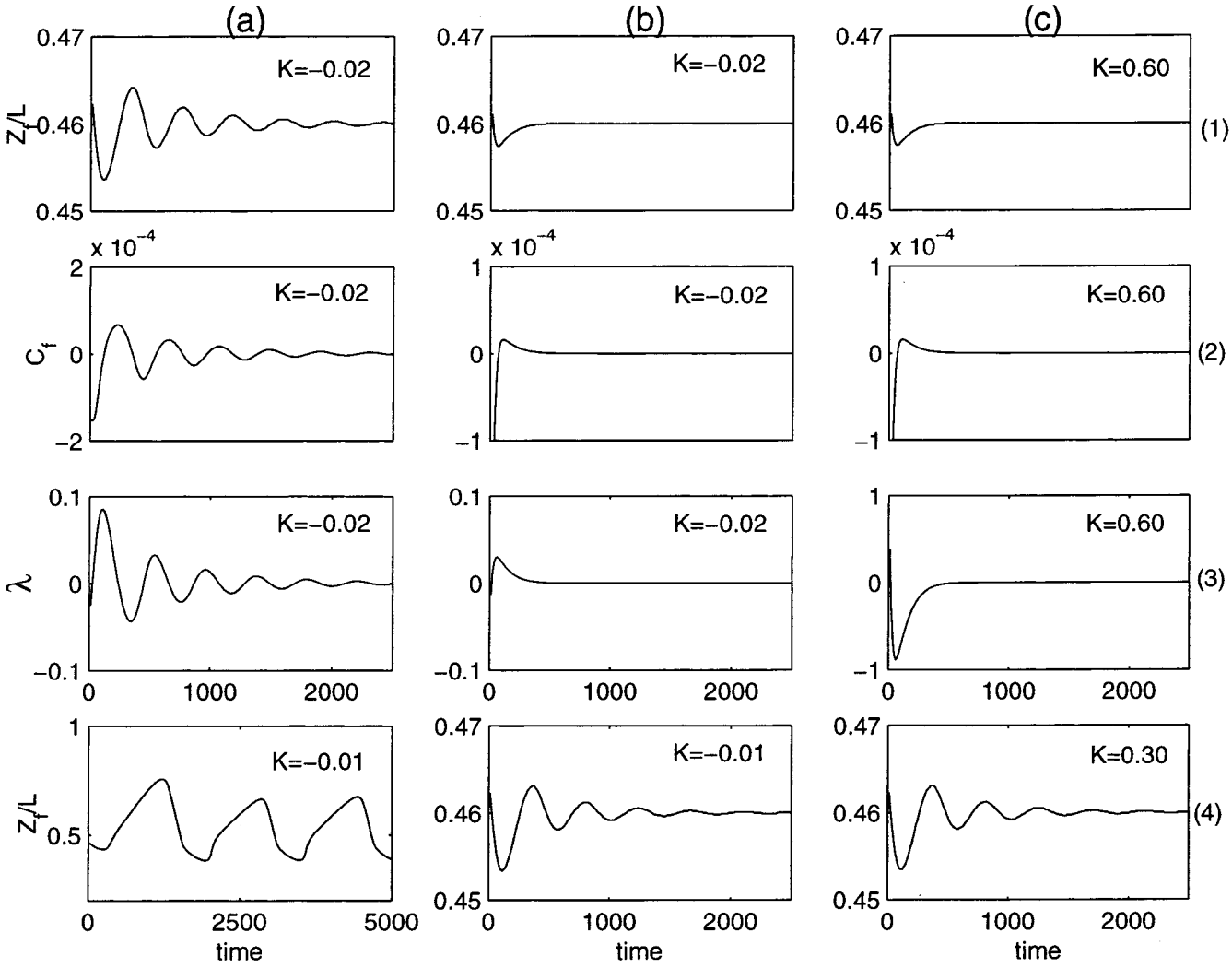

Figure 7. Testing of theory in simulations of a detailed adiabatic reactor model (eq 2). Response of the closed-loop system to an initial perturbation (shifting the front position $Z_{fs}|L = 0.46$ to $Z_f|L = 0.465$) using V control (a), x_{in} control (b), and B control (c). The figure presents the front position (Z_f; rows 1 and 4), the front velocity (c_f; row 2), and the control variable (λ; row 3). The gain coefficients K are shown. (Other parameters: $Le = 100$, $Da = 0.0465$, $Pe_T = 50$, $Pe_C = 6.25$, $B = 30$, $\gamma = 20$, $\epsilon = 5 \times 10^{-5}$, $a_\theta = 80$, and $b_\theta = 100$.)

with σ_i, $i = 1$, ..., etc., satisfying the equation $\tanh(\sigma_i L) = V\sigma_i/(\sigma_i^2 - 0.25V^2)$.

The last equation differs from the one obtained in works in refs 1 and 8 only because $L \neq 1$ in our case.

Substituting eq A3 into eqs A1 and A2 with $\lambda(t) = K\bar{y}(Z^*,t)$ and integrating with a weighted eigenfunction $\phi_j^a(z)$ result in the infinite system of ODE

$$\dot{a}_i = -\lambda_i a_i + \sum_m J_{im} a_m + b_i + K\int_0^L \sum_m a_m \phi_m(Z^*)\, \phi_i^a(z)\, dz \quad \text{(A7)}$$

$$\dot{b}_i = -\epsilon(\gamma a_i + b_i) \quad \text{(A8)}$$

where

$$J_{im} = \int_0^L \frac{\partial P}{\partial y}(y_s,\theta_s)\, \phi_m \phi_i^a\, dz, \quad i, m = 1, 2, ...$$

Denoting

$$h_m = \phi_m(Z^*) \quad \text{(A9)}$$

we can present the last term in eq A7 as

$$K\int_0^L \sum_m a_m \phi_m(Z^*)\, \phi_i^a(z)\, dz = K\sum_m a_m(t)\, h_m \int_0^L \Theta_i e^{-0.5Vz}\left[\cos(\sigma_i z) + \frac{V}{2\sigma_i}\sin(\sigma_i z)\right] dz$$

and rewrite eq A7 with the notation

$$d_i = \int_0^L \Theta_i e^{-0.5Vz}\left[\cos(\sigma_i z) + \frac{V}{2\sigma_i}\sin(\sigma_i z)\right] dz \quad \text{(A10)}$$

as follows:

$$\dot{a}_i = -\lambda_i a_i + \sum_m J_{im} a_i + b_i + K d_i \sum_m a_m(t)\, h_m \quad \text{(A11)}$$

ODEs (A11) and (A8) may be presented in the usual

vector−matrix form as the single-input single-output system

$$\begin{bmatrix}\dot{\mathbf{a}}\\ \dot{\mathbf{b}}\end{bmatrix}=\begin{bmatrix}-\mathbf{\Lambda}+\mathbf{J} & \mathbf{I}\\ -\epsilon\gamma\mathbf{I} & -\epsilon\mathbf{I}\end{bmatrix}\begin{bmatrix}\mathbf{a}\\ \mathbf{b}\end{bmatrix}+\begin{bmatrix}\mathbf{d}\\ \mathbf{O}\end{bmatrix}\lambda,\quad w=\mathbf{h}\begin{bmatrix}\mathbf{a}\\ \mathbf{b}\end{bmatrix} \tag{A12}$$

with the output feedback control

$$\lambda = Kw \tag{A13}$$

where $\mathbf{a}(t)=\mathbf{a}=(a_1, a_2, ...)^{\mathrm{T}}$, $\mathbf{b}(t)=\mathbf{b}=(b_1, b_2, ...)^{\mathrm{T}}$, $\mathbf{h}=(h_1, h_2, ..., 0, 0, ...)$, and $\mathbf{d}^{\mathrm{T}}=(d_1, d_2, ...)$ are the infinite-dimensional vectors and $\mathbf{\Lambda}=\mathrm{diag}(\lambda_1, \lambda_2, ...)$, $\mathbf{I}=\mathrm{diag}(1, 1, ...)$, $\mathbf{J}=[\mathbf{J}_{im}]$, $i, m = 1, 2, ...$, are infinite-dimensional matrices.

The problem of gain (K) design is transformed to the following problem: *For linearized infinite-dimensional ODEs system (A12), it is necessary to find the proportional output feedback control (A13) such that the closed-loop system is asymptotically stable.*

For control design we approximate ODE (A12) by a finite-dimensional truncated version. The order n of the truncated ODE system is evaluated by calculating the leading eigenvalue of the dynamic matrix of eq A12 for increasing N (number terms in the Galerkin series (A3); see Figure 2). It is evident that $n = 2N$. Calculation of the leading eigenvalues of the closed-loop system vs K is the best appropriate method for numerical evaluation of K_{cr}, the critical value that stabilizes the system (see Figure 3).

Control Design Based on Approximate Equation 31 (for Small $\epsilon \leq 0.01$). The design of the additive point sensor (manipulating λ) and the flow-rate (manipulating V) control strategies may be demonstrated by eq 31 with $y_{\mathrm{in}} = y_-$ without a loss of generality

$$\frac{\mathrm{d}Z_{\mathrm{f}}}{\mathrm{d}t}=-c_{\infty,V=0}+V-\alpha\frac{p-V}{V+p}\mathrm{e}^{-2pZ_{\mathrm{f}}}+\alpha\mathrm{e}^{-2p(L-Z_{\mathrm{f}})}$$

Here $\alpha=\alpha_-=\alpha_+$[5].

Consider the flow-rate control (eq 32) $V - V_0 = \tilde{k}(Z_{\mathrm{f}}(t) - Z_{\mathrm{s}})$, where Z_{s} is the steady-state point of eq A13 for assigned $V = V_0$. The analysis of the closed-loop linearized system with $\bar{Z}_{\mathrm{f}} = Z_{\mathrm{f}} - Z_{\mathrm{s}}$

$$\dot{\bar{Z}}_{\mathrm{f}}=2\alpha p\left(\frac{p-V}{p+V}\mathrm{e}^{-2pZ_{\mathrm{f}}}+\mathrm{e}^{-2p(L-Z_{\mathrm{f}})}\right)\Big|_{Z_{\mathrm{s}},V_0}\bar{Z}_{\mathrm{f}}+\left(1+\frac{2p\alpha}{(p+V)^2}\mathrm{e}^{-2pZ_{\mathrm{f}}}\right)\Big|_{Z_{\mathrm{s}},V_0}\tilde{k}\bar{Z}_{\mathrm{f}}$$

allows one to evaluate the critical value of $\tilde{k}$ that stabilizes the system. Then we will use the expression

$$\mathrm{abs}(K)=\mathrm{abs}(\tilde{k}(\mathrm{d}y/\mathrm{d}z)_{Z_{\mathrm{f}}}{}^{-1}) \tag{A14}$$

for evaluation of K in control (32). Assuming that perturbation displaces the front position without changing its shape, we can evaluate

$$\mathrm{d}y/\mathrm{d}z=(1-\gamma)[1-\tanh^2((z-Z_{\mathrm{f}})\sqrt{0.5(1-\gamma)})]/\sqrt{2} \tag{A15}$$

Using eq A15, we can compute the rough estimation of abs(K) (eq A14).

A similar estimation may be obtained for the additive point sensor.

Nomenclature

a = constant parameter (eq 35)
A = interphase surface per reactor volume
B = dimensionless exothermicity
$\mathbf{a} = \mathbf{a}(t)$ = infinite-dimensional state vector of a linearized lumped system (eq A12)
$\mathbf{b} = \mathbf{b}(t)$ = infinite-dimensional state vector of a linearized lumped system (eq A12)
C = constant (eq 31)
c = front velocity (eq 15)
C_{A} = key component concentration in the solid phase
$\mathbf{d}$ = infinite-dimensional input vector of a linearized lumped system (eq A12)
Da = Damkohler number
E = activation energy
f_1, f_2 = kinetic functions (eq 2)
$\mathbf{h}$ = infinite-dimensional output vector of a linearized lumped system (eq A12)
$\mathbf{I}$ = diag(1, 1, ...) = infinite-dimensional unity matrix (eq A12)
$\mathbf{J}$ = infinite-dimensional Jacobian matrix (eq A12)
K, $\tilde{k}$ = scalar gain coefficients
L = reactor length
Le = Lewis number
N = number of terms in the truncated Galerkin series
$n = 2N$ = order of the truncated lumping ODEs (eq 12)
p = eigenvalue of the linearized diffusion−reaction equation (eq 20)
Pe_{C}, Pe_{T} = Peclet numbers for mass and heat dispersion
$P(y,\theta,\lambda)$ = source function
q = variable of the PI regulator (eq 40)
$Q(y,\theta)$ = source function
R = universal gas constant
t = time
T = temperature
V = dimensionless convective velocity (eqs 1a and 13)
$w = w(t)$ = output (scalar) of a linearized lumped system (eq A12)
x = dimensionless concentration
y = dimensionless temperature
$\bar{y} = y - y_{\mathrm{s}}$ = deviation of y (eq A1)
z, ξ = dimension and dimensionless axial coordinates
Z^* = sensor position
α = parameter (eq 20)
β_{C}, β_{T} = dimensionless fluid-to-wall transport coefficients
γ = constant parameter (eq 35)
δ = parameter in eq 2
ϵ^{-1} = time scale (eq 1b)
ζ = coordinate moving with the front (eq 15)
$\theta = \theta(z,t)$ = state variable (catalytic activity)
$\bar{\theta} = \theta - \theta_{\mathrm{s}}$ = deviation of θ (eq A2)
Θ_i = constant (eq A6)
τ = dimensionless time
$\mathbf{\Lambda} = \mathrm{diag}(\lambda_1, \lambda_2, ...)$ = infinite-dimensional diagonal matrix (eq A12)
$\lambda = \lambda(t)$ = control variable
λ_i = eigenvalues of the linear operator
ϕ_i, ϕ_i^{a} = eigenfunctions and adjoint eigenfunctions of the linear operator (eqs A4 and A5)
$\langle \cdot, \phi_i \rangle$ = integral with weight function ϕ_i

Subscripts

s = at steady state
sf = at the steady front position
f, f_1, f_2 = at the front position
∞ = unbounded system

+, − = values in the upper and low states, respectively
in = at the inlet
w = at the wall

Literature Cited

(1) Ray, W. H. *Advanced Process Control*; McGraw-Hill: New York, 1981.

(2) Panfilov, V.; Sheintuch, M. Using Weighted Global Control for Stabilizing Pattern States. *Chaos* **1999**, *9* (1), 78.

(3) Smagina, Ye.; Nekhamkina, O.; Sheintuch, M. Stabilization of Front in Reaction−Diffusion System: Application of Gershgorin Theorem. *Ind. Eng Chem. Res.*, in press.

(4) Panfilov, V.; Sheintuch, M. Control Strategies for Front Stabilization in a Tubular Reactor model. *AIChE J.* **2001**, *47*, 187

(5) Sheintuch, M.; Nekhamkina, O. Analysis of Front-Interaction and Control in Stationary Patterns in Reaction−Diffusion Systems. *Phys. Rev. E* **2001**, *63*, 56120.

(6) Georgakis, C.; Aris, R.; Amundson, N. R. Studies in the Control of Tubular Reactors. I, II, III. *Chem. Eng. Sci.* **1977**, *32*, 1359.

(7) Shvartsman, S. Y.; Kevrekidis, I. G. Nonlinear Model Reduction for Control of Distributed Systems: a Computer-Assisted Study. *AIChE J.* **1998**, *44*, 1579.

(8) Christofides, P. D.; Daoutidis, P. Nonlinear Control of Diffusion−Convection−Reaction Processes. *Comput. Chem. Eng.* **1996**, *20, S1071.*

(9) Doyle, F. J.; Budman, H.; Morari, M. 'Linearizing' controller design for a packed-bed reactor using a low-order wave propagation. *Ind. Eng. Chem. Res.* **1996**, *35*, 3567.

(10) Christofides, P. D. Robust Control of Parabolic PDE system. *Chem. Eng. Sci.* **1998**, *53* (16), 2949.

(11) Christofides, P. D.; Daoutidis, P. Finite-Dimensional Control of Parabolic PDE System using Approximate Inertial Manifolds. *J. Math. Anal. Appl.* **1997**, *216*, 398.

(12) Fife, P. C. *Mathematical Theory of Reacting and Diffusing Systems*; Springer-Verlag: Berlin, 1979.

(13) Mikhailov, A. S. *Foundations of Synergetics. I*: *Distributed Active Systems*; Springer-Verlag: Berlin, 1994.

(14) Sheintuch, M.; Nekhamkina, O. Pattern Formation in Homogeneous and Heterogeneous Reactor Models. *Chem. Eng. Sci.* **1999**, *54*, 4535.

(15) Nekhamkina, O. A.; Rubinstein, B. Y.; Sheintuch, M. Spatiotemporal Patterns in Thermokinetic Models of Cross-Flow Reactors. *AIChE J.* **2000**, *46*, 1632.

(16) Nekhamkina, O. A.; Rubinstein, B. Y.; Sheintuch, M. Spatiotemporal Patterns in Models of Cross-Flow Reactors. Regular and Oscillatory Kinetics. *Chem. Eng. Sci.* **2001**, *56*, 771.

(17) Sheintuch, M. Spatiotemporal Structures of Controlled Catalytic Wires. *Chem. Eng. Sci.* **1989**, *44*, 1081.

(18) Middya, U.; Luss, D.; Sheintuch, M. Spatiotemporal Motions due to Global Interaction. *J. Chem. Phys.* **1993**, *100*, 3568.

(19) Burghardt, A.; Berezowski, M.; Jacobsen, E. W. Approximate Characteristics of a Moving Temperature Front in a Fixed-Bed Catalytic Reactor. *Chem. Eng. Process* **1999**, *38*, 19.

(20) Puszynski, J.; Degreve, J.; Hlavacek, V. Modeling of Exothermic Solid−Solid Noncatalytic Reactions. *Ind. Eng. Chem. Res.* **1987**, *26*, 1424.

(21) Frank-Kamenetski, D. A. *Diffusion and Heat Exchange in Chemical Kinetics*; Princeton University Press: Princeton, NJ, 1955.

(22) Sheintuch, M.; Shvartsman, S. Y. Spatiotemporal Patterns in Catalytic Reactors. *AIChE J.* **1996**, *42* (4), 1041.

Received for review August 27, 2001
Revised manuscript received January 9, 2002
Accepted January 24, 2002

IE0107082